

Improving COVID-19 chest X-ray classification via attention-based learning and fuzzy-augmented data diversity

Girish Shyadanahalli Cheluvvaraju^{1,2}, Jayasri Basavapatna Shivasubramanya³

¹Department of Information Science and Engineering, GSSS Institute of Engineering and Technology for Women, Mysuru, India

²Department of Computer Science and Engineering, Visvesvaraya Technological University, Belagavi, India

³Department of Computer Science and Engineering, The National Institute of Engineering, Mysuru, India

Article Info

Article history:

Received Jun 13, 2025

Revised Aug 13, 2025

Accepted Sep 11, 2025

Keywords:

Chest X-ray imaging

COVID-19 detection

Deep learning

Fuzzy logic augmentation

Hybrid attention mechanism

Uncertainty-aware ensemble

ABSTRACT

This paper presents a hybrid deep learning (DL) framework that combines model-level and data-level enhancements to improve classification performance without compromising clinical relevance. The proposed framework consisted of an EfficientNetB0 model with a hybrid attention module, which focused attention both spatially and channel-wise, and a VGG-16 model that was trained on training data augmented using a fuzzy-logic-based contrast and brightness enhancement. The attention module focused the model by recalibrating the features in an adaptive manner. The fuzzy-logic augmentation increased data diversity while maintaining the anatomical fidelity of the medical image domain. In addition, an uncertainty-aware ensemble approach was utilized to combine both models' predictions, which considered model confidence and entropy of the predictions, to enhance the reliability of the predictions. The proposed framework achieves a classification accuracy of 99.6%, outperforming several existing approaches.

This is an open access article under the [CC BY-SA](#) license.



Corresponding Author:

Girish Shyadanahalli Cheluvvaraju

Department of Information Science and Engineering

GSSS Institute of Engineering and Technology for Women

KRS Road, Mysuru, Karnataka 570016, India

Email: girishsadanahalli1127@gmail.com

1. INTRODUCTION

The COVID-19 pandemic has increased the demand for rapid, reliable and scalable diagnostic tools [1]. Although immediate reverse transcription polymerase chain reaction (RT-PCR) still remains the standard for COVID-19 testing [2], it has limitations such as low sensitivity, slow speed and dependence on specialized laboratory infrastructure [3]. Chest X-ray (CXR) imaging provides a widely accessible and affordable option for early screening and monitoring, especially in low-resource settings [4]. The recent advancements in deep learning (DL), have opened up new prospects for reaching reliable and automated CXR interpretation [5], [6]. However, it is challenging to meet the requirements of the real-world deployment due to various issues such as: i) most publicly available COVID-19 CXR datasets are small and imbalanced for models to generalize [7]; ii) expression of disease varied and thus compromised consistency of feature extraction [8]; iii) some form of preprocessing can negate diagnostic certainty by transforming clinical markers [9]; and iv) most non-confirming considerations were determinants. In the literature, there is a wide adoption of convolutional neural networks (CNNs) towards detecting COVID-19 from CXR images, due to their effectiveness in automatic feature extraction and effective disease classification [10], [11]. There are also many studies towards implementing transfer learning using pre-trained architectures such as ResNet, VGG, EfficientNet, and DenseNet has become a common strategy [12]. Ismael and Şengür [13] used pre-

trained ResNet-50 and VGG-16 for deep feature extraction and then used a support vector machine (SVM) classifier, achieving an accuracy of 94.7%. Similarly, Heidari *et al.* [14] tried to enhance the VGG-16 feature learning by using histogram equalization and bilateral filtering on the input CXRs, and achieved 94.5% multi-class accuracy. The work of Monshi *et al.* [15] focuses on improving the performance of VGG-19 and ResNet-50 using data augmentation and hyperparameter tuning. Rao *et al.* [16] presented a combined approach of a custom CNN with a quantum classifier and achieved 98.1% accuracy, and Hilali-Jaghdam *et al.* [17], who combined median filtering with a parent optimization algorithm for DenseNet feature extraction and autoencoder-based classification. Although many schemes have been introduced, but most CNN-based methods are often affected by spatial irregular features as reported by Kiziloluk *et al.* [18], such as ground-glass opacity due to fixed convolutional filters and uniform sampling. To address this issue, optimization approach by Gülmez [19] and attention-based methods have been explored by Cheng *et al.* [20], where the authors have proposed a self-attention network for noisy image conditions. Similarly, Roy *et al.* [21] developed a squeeze and excitation (SE) network with both spatial and channel attention (CA) mechanisms. There is also work towards applying a transformer-based model by Oltu *et al.* [22], where a visual transformer is combined with DenseNet201 to capture long-range dependencies and local features. In the same direction, Bayoudh *et al.* [23] applied enhanced histogram equalization on self-features whereas Schaffta *et al.* [24] used texture rectified cross-attention to improve classification performance. In the work of Sayeed *et al.* [25], the authors have introduced a dual-path framework that combines a residual U-Net for segmentation with two attention-based ensemble classifiers. From the reviewed literature, it is clear that transfer learning based on pre-trained CNN models remains the primary method for COVID-19 detection. Although pre-processing and data augmentation strategies have been applied to improve performance, overly complex or invasive pre-processing can distort important clinical image details. Attention mechanisms have also been studied, but in most cases, attention maps cannot be dynamically adjusted during training, resulting in sub-optimal localization of important disease regions. The significant research gaps are identified as presented here:

- Many existing studies are much dependent on the direct adoption of the pre-trained CNNs model without architecture customization, or pre-processing, enhancement, or parameter tuning.
- In the literature, the attention mechanism is used but not dynamically adjusted, which can lead to the loss of spatial channel focus and often increases model complexity.
- Most models lack uncertainty estimates and produce deterministic predictions without confidence measures, which can be risky for clinical applications where reliability is crucial.

This paper introduces a hybrid learning system for COVID-19 detection using CXR images, where a lightweight attention-enhanced EfficientNet model is combined with a VGG-16 model trained using fuzzy-based data augmentation. The novelty of the proposed methodology is that it addresses the suboptimal feature localization so that the model preserves clinical relevance and improves sensitivity to complex lung patterns. The uncertainty-aware ensemble adds a layer of reliability, making the system more suitable for real-world clinical applications. The novel contribution of this paper is highlighted as follows:

- This study develops a custom channel–spatial attention (SA) module that dynamically adapts during training to enhance the localization of disease-specific lung abnormalities.
- A context-aware enhancement technique is proposed using fuzzy logic as a data augmentation that improves both local (region-wise) and global image quality in the training set.
- An uncertainty-aware ensemble strategy is proposed that integrates model confidence and entropy-based uncertainty into the weighting process to improve prediction reliability and reduce risk in high-stakes clinical decisions.

2. METHOD

The primary aim of this work is to develop a reliable and effective predictive model for the detection of COVID-19 from CXR images. The proposed system introduces a hybrid learning framework that integrates attention-enhanced and data-augmented CNNs to improve both feature representation and generalisation capability of the classification models, thereby preserving the diagnostic integrity of the input data. The entire modelling of the proposed system adopts analytical research methodology, which can be divided into four phases, viz.: i) preprocessing, ii) EfficientNetB0 with a hybrid attention module, iii) VGG-16, trained on a fuzzy-augmented version of the training set, and iv) uncertainty-based ensemble learning. Figure 1 outlines the design and workflow process of the proposed system aimed to balance predictive accuracy, generalisation, and clinical relevance in the context of COVID-19 and other chest infection detection using CXR images.

This study aims to analyse three most common viral CXR conditions, such as COVID-19, viral pneumonia, and normal conditions, using the benchmarked dataset, i.e., COVID-19 radiology database [26],

which contains approximately 15,000 CXR images. The study considered a preprocessing module where all the images in the dataset were resized to 224×224 pixels to meet the input requirements of EfficientNetB0 and VGG-16. The proposed study then divided the dataset based on a stratified 80:10:10 ratio to accomplish proportional representation of classes along training, validation, and test sets, and prevented data leakage by ensuring that images are assigned to only one subset.

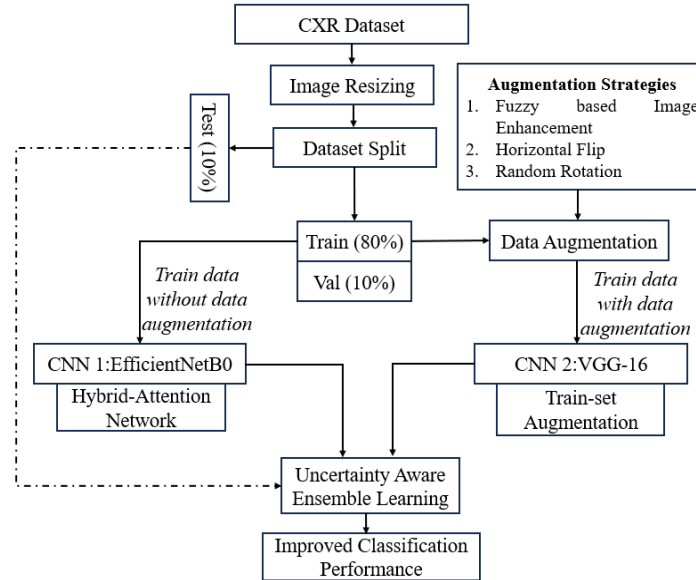


Figure 1. Architecture of the proposed framework for COVID-19 classification

2.1. EfficientNet with hybrid attention

The first core module of the proposed system is the convolutional operation using EfficientNetB0 CNN architecture, which is selected for its parameter efficiency and ability to extract high-quality features from medical images. This model takes the input image $I \in \mathbb{R}^{W \times H}$, which after standard convolutional processing, produces a feature map $F \in \mathbb{R}^{W \times H \times C}$, where W , H , and C represent the width, height, and number of feature channels (depth), respectively. In order to improve the network's ability to focus on disease-relevant regions such as ground-glass opacities and lung consolidations, a hybrid attention module (H-Atten) is developed and integrated into EfficientNetB0 architecture, which consists of two consecutive sub-modules, namely CA and SA, applied sequentially to recalibrate the feature map.

In H-Attention, the feature map F obtained from the last convolutional layer is first processed via a mean pooling operation (1), considering its spatial dimensions to generate a compressed vector F'_c that capture the global context of each channel. In order to perform selective focus on important channels a bottleneck transformation is considered, where 1×1 convolutional layer is applied over F'_c to reduce channel dimensionality F_{red} using a reduction ratio r followed by a rectified linear unit (ReLU) activation. The vector F_{red} that represent the activation (importance), which means the channel with higher activations will have stronger feature representation of the input data. Afterwards, the original channel dimension is restored by applying second 1×1 convolution layer over F_{res} (2), so that the full range of information from the initial input is used in the final feature recalibration process. The next operation is carried towards obtaining CA weights using the SoftMax function over an input vector F_{res} (3). The reason behind using SoftMax is that we need to compute a probability distribution that shows the relative importance of each channel in F_{res} and accordingly assigns a higher weight to channels with strong activations. These weights are applied to the original feature map via element-wise multiplication to get the final CA map (4).

$$F'_c = \frac{1}{W \times H} \sum_{i=1}^W \sum_{j=1}^H F(i, j, c), \forall c \in [1, C] \quad (1)$$

$$F_{red} = \text{ReLU}(W_1 F' + b_1), \text{ and } F_{res} = W_2 F_{red} + b_2, \text{ where } W_1 \in \mathbb{R}^{C \times \frac{C}{r}}; W_2 \in \mathbb{R}^{\frac{C}{r} \times C} \quad (2)$$

$$A_c(c) = \frac{\exp(F_{res}(c))}{\sum_{k=1}^C \exp(F_{res}(k))}, \forall c \in [1, C] \quad (3)$$

$$F_{CA}(i, j, c) = F(i, j, c) \cdot A_c(c) \quad (4)$$

In order to capture spatial saliency map, the proposed study aggregate across all channels at each spatial location (5). Then, a sigmoid activation is applied to generate SA weights (6). These weights are broadcasted across all channels and applied to the channel-attended map, which generates a final output, i.e., recalibrated feature map F'' (7), which further passed to the dense layer for the classification. The detailed network architecture with parameter specifications is provided in Table 1, followed by the internal layers and parameters of the proposed H-Attention module illustrated in Figure 2.

$$F_{sum}(i, j) = \sum_{c=1}^C F_{CA}(i, j, c) \quad (5)$$

$$A_s(i, j) = \sigma(F_{sum}(i, j)) = \frac{1}{1 + e^{-F_{sum}(i, j)}} \quad (6)$$

$$F'' = F(i, j, c) \otimes A_W(i, j) \quad (7)$$

Table 1. Illustrates network architecture and parameter specifications

Component	Output shape	Param #	Description
Input layer	(None, 224, 224, 3)	0	Input RGB image
EfficientNetB0	(None, 7, 7, 1280)	4,049,571	Pretrained backbone (without top), used for feature extraction
H-Atten model	(None, 7, 7, 1280)	206,160	Custom channel-SA block with:– GAP– 1×1 Conv (\downarrow channels)– ReLU– 1×1 Conv (\uparrow channels)– SoftMax + Sigmoid
Global avg pooling	(None, 1280)	0	Reduces spatial dimensions to a vector per channel
Batch normalization	(None, 1280)	5,120	Normalizes activations after pooling
Dense (fully connected)	(None, 256)	327,936	Activation: ReLU; L1/L2 regularization
Dropout	(None, 256)	0	Dropout with rate=0.45 for regularization
Output layer	(None, 3)	771	Final classification layer with SoftMax

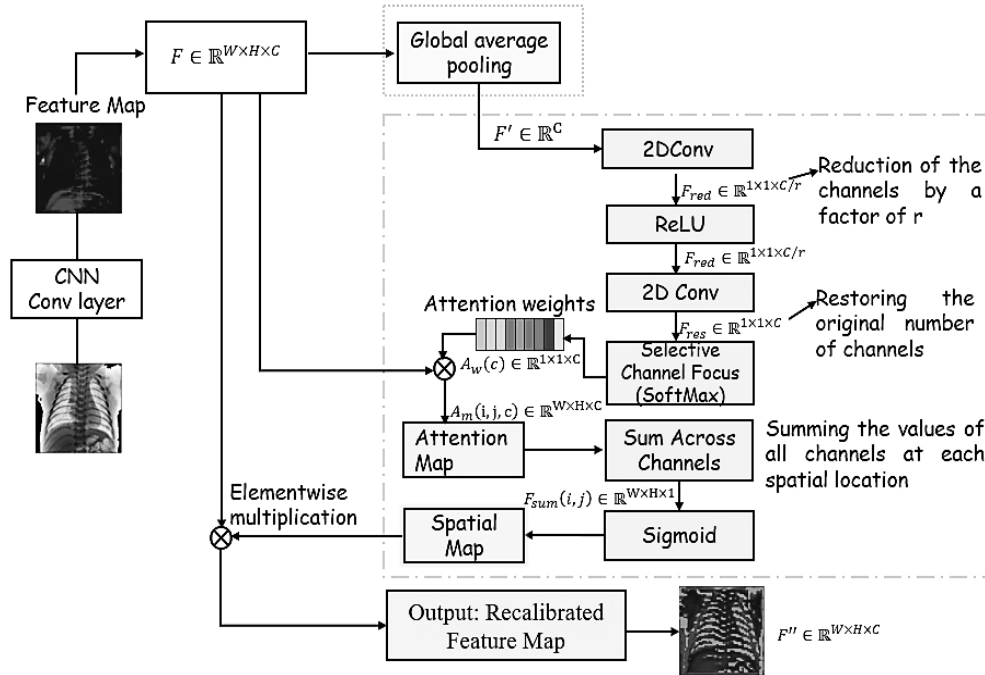


Figure 2. Architecture of the proposed H-Atten model for enhanced feature map representation

The proposed H-Atten module enhances EfficientNetB0 by sequentially applying channel and spatial recalibration, allowing the network to focus on clinically relevant lung regions more effectively. The adopted approach of selective channel focus in the attention mechanism improves the detection of hidden or understated COVID-19-related patterns, such as ground-glass opacity, and eliminates irrelevant background

noise. The proposed H-Atten model offers better feature representation to the CNN model towards achieving higher classification performance without significantly increasing the computational complexity.

2.2. VGG-16 with fuzzy-based image augmentation

The second module in the proposed framework is based on VGG-16 CNN architecture, which is trained specifically on a high-level training dataset. To improve the diversity, contrast quality, and generalisation of this model, we apply a fuzzy logic-based image enhancement technique that adaptively adjusts the brightness and contrast of each region to enhance important diagnostic details, such as hiding shadows or low-contrast lesions, while preserving the semantic structure of the image. The enhancement process considers dividing each input grayscale CXR image $I \in \mathbb{R}^{W \times H}$ into overlapping blocks of size $b \times b$, where $b = 32$ and the overlap is 50%. For each block B_k three statistical features are computed such as mean brightness μ_k , and local contrast σ_k using (8). Then it computes edge details ϵ_k using the mean Sobel gradient using (9), where ∇B_k is the Sobel response at location (i, j) .

$$\mu_k = \frac{1}{b^2} \sum_{i=1}^b \sum_{j=1}^b B_k(i, j) \text{ and } \sigma_k = \sqrt{\frac{1}{b^2} \sum_{i=1}^b \sum_{j=1}^b (B_k(i, j) - \mu_k)^2} \quad (8)$$

$$\epsilon_k = \frac{1}{b^2} \sum_{i=1}^b \sum_{j=1}^b |\nabla B_k(i, j)| \quad (9)$$

2.2.1. Fuzzification and membership functions

The obtained features μ_k , σ_k , and ϵ_k further serve as inputs to a Mamdani-type fuzzy inference system, where each input is represented by linguistic variables (e.g., low, optimal, high for brightness, and contrast; low, medium, and high for edge detail) modelled with trapezoidal or triangular membership functions. The system produces output decisions, viz.: i) brightness adjustment $\Delta_{\mu_k} \in [-50, 50]$ and ii) contrast adjustment $\alpha_k \in [0.5, 1.5]$. This fuzzification process ensures that the enhancement decisions are compatible with local image statistics and clinically relevant texture information. Table 2 highlights the fuzzification parameters and membership functions used in this study.

Table 2. Fuzzification parameters and membership functions

Input/output	Linguistic term	Membership function type	Parameter range
Brightness	Low	Trapezoidal	[0, 0, 110, 120]
	Optimal	Triangular	[110, 120, 135]
	High	Trapezoidal	[130, 140, 255, 255]
Contrast	Low	Trapezoidal	[0, 0, 50, 55]
	Optimal	Triangular	[50, 60, 65]
	High	Trapezoidal	[60, 70, 127, 127]
Edge detail	Low	Trapezoidal	[0, 0, 0.02, 0.04]
	Medium	Triangular	[0.02, 0.04, 0.1]
	High	Trapezoidal	[0.04, 0.1, 1, 1]
Brightness adjustment	Decrease	Triangular	[-50, -25, 0]
	No change	Triangular	[-10, 0, 10]
	Increase	Triangular	[0, 25, 50]
Contrast adjustment	Decrease	Triangular	[0.5, 0.75, 1.0]
	No change	Triangular	[0.9, 1.0, 1.1]
	Increase	Triangular	[1.0, 1.25, 1.5]

2.2.2. Rule base and inference method

The fuzzy rule base consists of 27 rules (3 brightness×3 contrast×3 edge detail combinations) to map specific input conditions to brightness and contrast adjustments. This concise but comprehensive design covers all possible combinations of local image statistics. The estimation is done using the Mamdani min-max method, and the output is defuzzified using the centroid technique to obtain smooth and interpretable enhancement values. The following are representative sample examples of the rule set used:

- Rule 1: IF brightness is low AND contrast is low THEN increase brightness AND increase contrast.
- Rule 14: IF brightness is optimal AND contrast is optimal THEN no change.
- Rule 27: IF brightness is high AND contrast is high THEN decrease brightness AND decrease contrast.

2.2.3. Parameter tuning and reconstruction

In the proposed work, the thresholds considered for membership functions were determined empirically by analysing the histogram statistics of 500 randomly sampled CXR images from the training set. Basically, the edge detail thresholds were tuned to detect minute ground-glass opacities without amplifying

noise. The resulting outputs μ_k and α_k are then used to generate the enhanced block B'_k and to ensure smooth transitions between blocks, a Hanning window operation H_k is applied to each B'_k and all processed blocks are accumulated using a weighted sliding window approach to the final enhanced image $I' \in \mathbb{R}^{W \times H}$ using (10).

$$B'_k = \alpha_k \cdot (B_k - \mu_k) + (\mu_k - \Delta_{\mu_k}) \text{ and } I'(x, y) = \frac{\sum_k H_k(x, y) \cdot B'_k(x, y)}{\sum_k H_k(x, y)} \quad (10)$$

It is also to be noted that the proposed fuzzy-based augmentation is applied only to the training set to preserve the clinical authenticity of the validation and test images. Figure 3 presents the visual analysis of the proposed fuzzy-based image enhancements. The use of fuzzy logic enables context-aware enhancement, where image regions with poor contrast or brightness are selectively enhanced without globally altering the image. Apart from this, the proposed augmentation scheme considers two additional operations, such as random rotation and horizontal flipping of images in the training set.

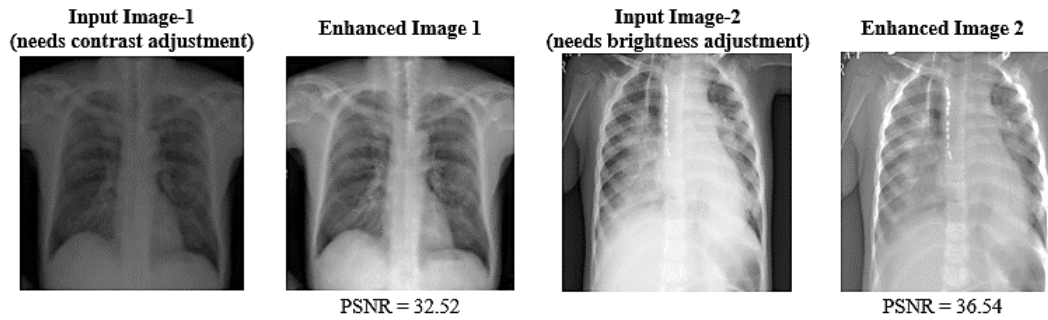


Figure 3. The visual outcome of the proposed fuzzy-based image enhancements

2.3. Uncertainty aware ensemble learning

In order to achieve enhanced predictive outcomes and minimise misclassification rate, the proposed study introduces an uncertainty-aware ensemble learning scheme that incorporates confidence and prediction uncertainty of both models and fuses their predictions towards offering a practical balance between accuracy, trust, and transparency. The proposed methodology considers an input image x_i and the prediction output from model $j \in \{1, 2\}$ be represented as a probability vector $P_j(x_i) = [p_{j1}, p_{j2} \dots p_{jK}]$, where K is the number of classes, and for each model prediction, the maximum class probability is extracted to define model confidence $c_{ji} \leftarrow \max(P_j(x_i))$. In order to compute stability and ranking behaviour, the confidence score of the models is passed through a composite ranking function R_{ji} , which reflects both the strength and reliability of the model's prediction for the image x_i . The uncertainty of each prediction is then estimated using Shannon entropy over the predicted probability distribution using (11):

$$\alpha_i = -\sum_{k=1}^K p_k \log(p_k), \text{ where } p_k = P_j(x_i)_k \quad (11)$$

where, a higher entropy α_i represents more uncertainty in the model's decision. To penalise such uncertain predictions, a penalty factor is introduced that down-weights predictions with higher entropy. Additionally, a weight $w \in [0, 1]$ is assigned to each model based on its validation accuracy on a held-out dataset to ensure that more reliable models contribute more to the final decision. The final fused prediction score for class k is computed by combining model-specific weights, confidence scores, and uncertainty penalties such that: $F_{jk} = w_j \cdot R_{ji} \cdot (1 - \alpha_i) \cdot P_j(x_i)_k$. Finally, the ensemble outputs from all models are aggregated, and the class label corresponding to the highest combined score is selected as the final predicted label such that: $\hat{y}_i = \arg \max_k \sum_{j=1}^M F_{jk}$, where $M = 2$, i.e., is the number of models in the ensemble.

The proposed scheme not only allows the system to aggregate predictions but also adaptively weights them based on the confidence and reliability of the inputs. As a result, the system is less sensitive to errors in a single model and better able to meet clinical reliability requirements. From an optimisation perspective, the proposed uncertainty-aware ensemble mechanisms act as a built-in loss regularizer by penalising high-entropy (low-reliability) predictions, thereby reducing their influence on the final decision. Similar to confidence-weighted cross-entropy, it also enhances the reliability and stability in the prediction

even in highly uncertain scenarios, which is critical for clinical COVID-19 testing, as overconfidence errors can be detrimental. The proposed schemes ensure that the system maintains a balance between accuracy, reliability, and interpretability.

3. RESULTS AND DISCUSSION

The implementation of the proposed system is carried out using the Python programming language on a Windows 11 64-bit system with an NVIDIA GTX 1650 GPU and 16 GB of RAM. The proposed framework is trained and evaluated on the benchmark dataset, namely the COVID-19 radiology database [26], which consists of approximately 15,000 CXR images with four classes (COVID-19, viral pneumonia, and normal). The training hyperparameters are selected based on the grid search technique on the validation set, where the batch size is selected as 32, as it offers a balance between convergence stability and GPU memory, and Adamax as an optimizer due to its robustness to sparse gradients and convergence stability. The results are evaluated using standard classification parameters such as accuracy, precision, recall, F1-score, and AUC. Table 3 shows the numerical outcomes for performance comparison with various baseline models.

Table 3. Comparative analysis with baseline CNNs

Model	Accuracy (%)	Precision (%)	Recall (%)	F1-score (%)
ResNet50	92	93	90	91
MobileNet	74	85	66	58
DenseNet	93	93	93	93
EfficientNetB0	96	92	96	94
VGG-16	94	94	93	93
EfficientNetB0 + H-Atten	98.3	97.9	98.5	98.2
VGG-16 + fuzzy augmentation	97.6	97.1	97.8	97.4
Proposed ensemble model	99.6	100	99	99

Table 3 presents a comparative assessment of the proposed learning models against various baseline CNN models widely adopted in the literature. It can be seen that the proposed ensemble model outperformed other CNN models with achieving a classification accuracy of 99.6% and an F1-score of 99%. Furthermore, EfficientNetB0 with the proposed H-Attention and VGG-16 with the proposed fuzzy data augmentation also outperform existing CNN models, thereby achieving a balanced and robust classification capability. In order to demonstrate the effectiveness of the proposed ensemble learning, Figures 4 and 5 demonstrate the confusion matrix and ROC curve analysis, respectively.

True Label	Covid-19	360	1	0
	Normal	1	1018	0
	Pneumonia	0	4	130
	Predicted Label	Covid-19	Normal	Pneumonia

Figure 4. Confusion matrix

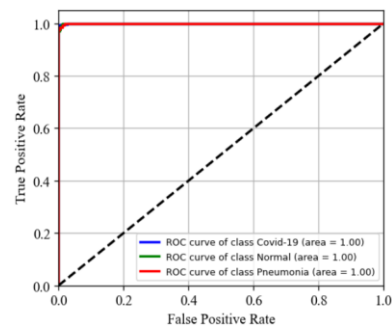


Figure 5. ROC curve analysis

Figure 4 illustrates the confusion matrix of the proposed ensemble model, which shows that only six data samples are misclassified out of a total of 1,514 test instances. The COVID-19 detection achieved a sensitivity of 99.72% and specificity of 99.91%, the normal cases achieved 99.90% sensitivity and 98.99% specificity, and pneumonia cases achieved 97.01% sensitivity and 100% specificity. The analysis shows lower false positive rate than the previous methods [27]-[30], along with balanced performance in terms of precision and recall than the similar existing works such as [31] (precision 96% and recall 95%), [32] (precision 94% and recall 97%), and [33] (precision and recall 97.48%). This analysis indicates that the proposed uncertainty-aware ensemble offers effective reliability in a multi-class classification task, which can also be seen in the analysis shown class-wise ROC curve in Figure 5. It can be seen that the proposed system is quite better at distinguishing all the classes, thereby achieving an AUC of 1.00, which highlights the model's excellent discrimination ability.

3.1. Discussion

Table 4 presents a comparative analysis with recent state-of-the-art (SOTA) methods in COVID-19 CXR classification, where a variety of techniques are applied by the researchers towards achieving higher performance in the classification task. However, none of the work has focused on optimizing the procedure or customizing the model for architectural engineering viewpoints. Very few works [34]–[36] have shown different work, but most of them are subjected to a common approach of model adoption where DL pipeline either by changing the base architecture or adding some known preprocessing, are considered which are already there in the literature. Hence, most existing approaches lack novelty and as a result, underperformed, whereas the proposed system, by fusing an H-Atten-driven model and a fuzzy-augmented trained model, outperformed all existing approaches with higher true positive and lower false positive rates.

Table 4. Comparative analysis with existing works

Ref	Dataset abbreviation	Classes	Techniques	Accuracy (%)
[27]	Public CXR-7000	COVID-19, pneumonia, tuberculosis, normal	DL+explainable artificial intelligence (XAI)	94
[28]	COVID-19 Rad-DB	COVID-19, normal, pneumonia	DL+transfer learning	91
[29]	COVID-19 Rad-DB	COVID-19, normal, pneumonia	DeTraC DNN	93
[30]	COVID-19 Rad-DB	COVID-19, normal, pneumonia	Attention guided ensemble	97.3
[31]	COVID-19 CXR	COVID-19, pneumonia, normal	Deep ensemble strategy	97
[32]	COVID + pneumonia CXR	COVID-19, pneumonia, normal	AI-driven knowledge distillation	96.34
[33]	Chest PA + Rad-DB	COVID-19, normal, pneumonia	CNN	97.48
[34]	COVID-19 Rad-DB	COVID-19, normal	SVM	93.4
[35]	COVID-19 Rad-DB	COVID-19, normal	Hist. Eq.+VGG19	95
[36]	Custom CXR	COVID-19, healthy, pneumonia	CNN-Attn+multi-level fusion	96.75
Proposed	COVID-19 Rad-DB	COVID-19, normal, pneumonia	EfficientNetB0+H-Atten	98.3
Proposed	COVID-19 Rad-DB	COVID-19, normal, pneumonia	VGG-16+fuzzy aug.	97.6
Proposed	COVID-19 Rad-DB	COVID-19, normal, pneumonia	Uncertainty aware ensemble	99.6

The existing works also achieved strong results, but also exhibit a few limitations. The DL and XAI framework introduced in [27] improved the interpretability but lacks the targeted preprocessing operation for better feature representation, whereas the COVID-ensemble in [28] boosts accuracy via transfer learning, but needs more optimization in feature learning and the generalization process. The model DeTraC in [29] addresses class imbalance but lacks attention for fine-grained localization, and the attention-guided ensembles introduced in [30] and deep ensembles in [31] enhance the robustness, but they adopted fixed fusion and ignored the vulnerability of overconfident errors. The knowledge distillation in [32] reduces the computational complexity but does not incorporate hybrid attention or advanced augmentation. The CNN in [33] is computationally efficient but limited by its single-backbone design, and similarly, the adoption of classical ML models in [34] is lightweight but cannot extract hierarchical features. The preprocessing-focused VGG19 [35] and CNN-attention fusion [36] improve performance but still lack adaptive, uncertainty-driven fusion. Our method addresses these gaps by introducing hybrid attention for region-focused features, fuzzy-based augmentation for local contrast and edge detail, and uncertainty-aware weighting for stable predictions, which showed an accuracy of 99.6% and outperformed the 91–97.48% range of prior works.

3.2. Limitations and clinical considerations

The proposed framework performs well in classifying multiple viral chest infections from input images, but it also has limitations. It is trained on a single publicly available CXR dataset, and the fuzzy logic augmentation is tuned to this dataset, which means that the thresholds used during inference need to be adjusted to avoid dataset-specific biases. The proposed model is also designed specifically for the CXR modality, but it can also be applied to other imaging modalities with slight modifications. Also, the hybrid attention mechanism and fuzzy augmentation approach introduce an increased training time, which we will optimize in future work. In terms of deployment, the framework is intended as a decision support tool, not a replacement for radiologists. The adoption of the proposed framework can help to optimize hospital workflows, it can priorities urgent cases, and improve resource allocation. However, the ethical and data privacy considerations are crucial for practical application. Though the dataset used in this work is publicly available, clinical deployment requires compliance with institutional review board (IRB) guidelines according to the health insurance portability and accountability act (HIPAA)/general data protection regulation (GDPR) to ensure secure handling of patient data.

4. CONCLUSION

This paper has proposed a novel hybrid DL framework for COVID-19 detection from CXR images based on the integration of a lightweight EfficientNetB0 model enhanced with a hybrid attention mechanism and a VGG-16 model trained on fuzzy logic-based augmented data. The integration of the outputs of both models was conducted with an uncertainty-aware ensemble strategy, which included model confidence, entropy-based uncertainty estimation, and validation-based dynamic weighting. The extensive experiments carried out on benchmark datasets showed that the proposed framework significantly outperformed baseline and SOTA models, and achieved 99.6% classification accuracy as well as excellent sensitivity and specificity. The experimental outcomes demonstrated the effectiveness of the proposed contributions, viz.: i) a hybrid attention mechanism to enhance region-specific features, ii) fuzzy enhancement to improve lesion visibility, and iii) uncertainty-aware fusion for robust decision making. The proposed system is designed to serve as a clinical decision support tool towards assisting radiologists in optimising case prioritisation and resource allocation. The future work will extend the current scope of the proposed work to multimodal datasets, including more disease classes, and make it more lightweight to enable broader clinical application.

FUNDING INFORMATION

The authors state that no funding was involved in this research.

AUTHOR CONTRIBUTIONS STATEMENT

This journal uses the Contributor Roles Taxonomy (CRediT) to recognize individual author contributions, reduce authorship disputes, and facilitate collaboration.

Name of Author	C	M	So	Va	Fo	I	R	D	O	E	Vi	Su	P	Fu
Girish Shyadanahalli	✓	✓	✓	✓	✓	✓		✓	✓	✓			✓	
Cheluvaraju														
Jayasri Basavapatna		✓				✓		✓	✓	✓	✓	✓		
Shivasubramanya														

C : Conceptualization

M : Methodology

So : Software

Va : Validation

Fo : Formal analysis

I : Investigation

R : Resources

D : Data Curation

O : Writing - Original Draft

E : Writing - Review & Editing

Vi : Visualization

Su : Supervision

P : Project administration

Fu : Funding acquisition

CONFLICT OF INTEREST STATEMENT

The authors state no conflict of interest.

DATA AVAILABILITY

The datasets used during this study are available from the corresponding author on request.

REFERENCES

- [1] S. A. Tabish, "COVID-19 pandemic: Emerging Perspectives and Future Trends," *Journal of Public Health Research*, vol. 9, no. 1786, pp. 19–26, 2020, doi: 10.4081/jphr.2020.17.
- [2] S. Abbas, A. Rafique, B. Abbas, and R. Iqbal, "Real-time polymerase chain reaction trends in COVID-19 patients," *Pakistan Journal of Medical Sciences*, vol. 37, no. 1, pp. 1–5, Dec. 2021, doi: 10.12669/pjms.37.1.3000.
- [3] A. Tahamtan and A. Ardebili, "Real-time RT-PCR in COVID-19 detection: issues affecting the results," *Expert Review of Molecular Diagnostics*, vol. 20, no. 5, pp. 453–454, May 2020, doi: 10.1080/14737159.2020.1757437.
- [4] E. Benmalek, J. Elmhamdi, and A. Jilbab, "Comparing CT scan and chest X-ray imaging for COVID-19 diagnosis," *Biomedical Engineering Advances*, vol. 1, p. 100003, Jun. 2021, doi: 10.1016/j.bea.2021.100003.
- [5] N. A. A. Majrashi, "The value of chest X-ray and CT severity scoring systems in the diagnosis of COVID-19: A review," *Frontiers in Medicine*, vol. 9, pp. 1–10, Jan. 2023, doi: 10.3389/fmed.2022.1076184.
- [6] A. Çinkoğlu, S. Bayraktaroglu, N. Ceylan, and R. Savaş, "Efficacy of chest X-ray in the diagnosis of COVID-19 pneumonia: comparison with computed tomography through a simplified scoring system designed for triage," *Egyptian Journal of Radiology and Nuclear Medicine*, vol. 52, no. 1, pp. 1–9, Dec. 2021, doi: 10.1186/s43055-021-00541-x.
- [7] L. Álvarez-Rodríguez, J. de Moura, J. Novo, and M. Ortega, "Does imbalance in chest X-ray datasets produce biased deep learning approaches for COVID-19 screening?," *BMC Medical Research Methodology*, vol. 22, no. 1, pp. 1–17, Dec. 2022, doi: 10.1186/s12874-022-01578-w.
- [8] H. Salarabadi, M. S. Iraj, M. Salimi, and M. Zoberi, "Improved COVID-19 Diagnosis Using a Hybrid Transfer Learning Model




Improving COVID-19 chest x-ray classification via attention-based ... (Girish Shyadanahalli Cheluvaraju)

- with Fuzzy Edge Detection on CT Scan Images,” *Advances in Fuzzy Systems*, no. 1, pp. 1–20, Jan. 2024, doi: 10.1155/2024/3249929.
- [9] M. A. A. Al-qaness *et al.*, “Chest X-ray Images for Lung Disease Detection Using Deep Learning Techniques: A Comprehensive Survey,” *Archives of Computational Methods in Engineering*, vol. 31, no. 6, pp. 3267–3301, Aug. 2024, doi: 10.1007/s11831-024-10081-y.
 - [10] S. Rajaraman, S. Sornapudi, P. O. Alderson, L. R. Folio, and S. K. Antani, “Analyzing inter-reader variability affecting deep ensemble learning for COVID-19 detection in chest radiographs,” *PLoS ONE*, vol. 15, pp. 1–32, Nov. 2020, doi: 10.1371/journal.pone.0242301.
 - [11] M. S. Iraj, “Combining predictors for multi-layer architecture of adaptive fuzzy inference system,” *Cognitive Systems Research*, vol. 53, pp. 71–84, Jan. 2019, doi: 10.1016/j.cogsys.2018.05.005.
 - [12] A. Khan, A. Sohail, U. Zahoora, and A. S. Qureshi, “A survey of the recent architectures of deep convolutional neural networks,” *Artificial Intelligence Review*, vol. 53, no. 8, pp. 5455–5516, Dec. 2020, doi: 10.1007/s10462-020-09825-6.
 - [13] A. M. Ismael and A. Şengür, “Deep learning approaches for COVID-19 detection based on chest X-ray images,” *Expert Systems with Applications*, vol. 164, pp. 1–11, Feb. 2021, doi: 10.1016/j.eswa.2020.114054.
 - [14] M. Heidari, S. Mirniaharikandehi, A. Z. Khuzani, G. Danala, Y. Qiu, and B. Zheng, “Improving the performance of CNN to predict the likelihood of COVID-19 using chest X-ray images with preprocessing algorithms,” *International Journal of Medical Informatics*, vol. 144, pp. 1–9, Dec. 2020, doi: 10.1016/j.ijmedinf.2020.104284.
 - [15] M. M. A. Monshi, J. Poon, V. Chung, and F. M. Monshi, “CovidXrayNet: Optimizing data augmentation and CNN hyperparameters for improved COVID-19 detection from CXR,” *Computers in Biology and Medicine*, vol. 133, pp. 1–13, Jun. 2021, doi: 10.1016/j.compbiomed.2021.104375.
 - [16] G. V. E. Rao, R. B., P. N. Srinivasu, M. F. Ijaz, and M. Woźniak, “Hybrid framework for respiratory lung diseases detection based on classical CNN and quantum classifiers from chest X-rays,” *Biomedical Signal Processing and Control*, vol. 88, p. 105567, Feb. 2024, doi: 10.1016/j.bspc.2023.105567.
 - [17] I. Hilali-Jaghdam *et al.*, “Towards COVID-19 detection and classification using optimal efficient Densenet model on chest X-ray images,” *Alexandria Engineering Journal*, vol. 101, pp. 136–146, Aug. 2024, doi: 10.1016/j.aej.2024.05.073.
 - [18] S. Kiziloluk, E. Sert, M. Hammad, R. Tadeusiewicz, and P. Plawiak, “EO-CNN: Equilibrium Optimization-Based hyperparameter tuning for enhanced pneumonia and COVID-19 detection using AlexNet and DarkNet19,” *Biocybernetics and Biomedical Engineering*, vol. 44, no. 3, pp. 635–650, Jul. 2024, doi: 10.1016/j.bbe.2024.06.006.
 - [19] B. Gülmöz, “A new multi-objective hyperparameter optimization algorithm for COVID-19 detection from x-ray images,” *Soft Computing*, vol. 28, no. 19, pp. 11601–11617, Oct. 2024, doi: 10.1007/s00500-024-09872-z.
 - [20] B. Cheng, R. Xue, H. Yang, L. Zhu, and W. Xiang, “DPN-SENet: A self-attention mechanism neural network for detection and diagnosis of COVID-19 from chest x-ray images,” *Research Square*, Jun. 14, 2021, doi: 10.21203/rs.3.rs-577494/v1.
 - [21] A. G. Roy, N. Navab, and C. Wachinger, “Recalibrating Fully Convolutional Networks With Spatial and Channel ‘Squeeze and Excitation’ Blocks,” *IEEE Transactions on Medical Imaging*, vol. 38, no. 2, pp. 540–549, Feb. 2019, doi: 10.1109/TMI.2018.2867261.
 - [22] B. Oltu, S. Güney, S. E. Yuksel, and B. Dengiz, “Automated classification of chest X-rays: a deep learning approach with attention mechanisms,” *BMC Medical Imaging*, vol. 25, no. 1, pp. 1–16, Mar. 2025, doi: 10.1186/s12880-025-01604-5.
 - [23] K. Bayouhdh, F. Hamdaoui, and A. Mtibaa, “C-Hybrid-NET: A self-attention-based COVID-19 screening model based on concatenated hybrid 2D-3D CNN features from chest X-ray images,” *Multimedia Tools and Applications*, vol. 84, no. 19, pp. 21829–21861, Jul. 2025, doi: 10.1007/s11042-024-19800-w.
 - [24] C. B. J. Schafftar, A. Radhakrishnan, and C. E. Prema, “A novel optimized machine learning approach with texture rectified cross-attention based transformer for COVID-19 detection,” *Biomedical Signal Processing and Control*, vol. 101, p. 107136, Mar. 2025, doi: 10.1016/j.bspc.2024.107136.
 - [25] A. Sayeed *et al.*, “An effective screening of COVID-19 pneumonia by employing chest X-ray segmentation and attention-based ensemble classification,” *IET Image Processing*, vol. 18, no. 9, pp. 2400–2416, Jul. 2024, doi: 10.1049/ipr2.13106.
 - [26] T. Rahman, M. Chowdhury, and M. Chowdhury, “COVID-19 Radiography Database,” Kaggle. [Online]. Available: <https://www.kaggle.com/datasets/tawsifurrahman/covid19-radiography-database>. (accessed: May. 12, 2025.)
 - [27] M. Bhandari, T. B. Shahi, B. Siku, and A. Neupane, “Explanatory classification of CXR images into COVID-19, Pneumonia and Tuberculosis using deep learning and XAI,” *Computers in Biology and Medicine*, vol. 150, pp. 1–12, Nov. 2022, doi: 10.1016/j.compbiomed.2022.106156.
 - [28] X. Liu, W. Wu, J. Chun-Wei Lin, and S. Liu, “A Deep Learning Model for Diagnosing COVID-19 and Pneumonia through X-ray,” *Current Medical Imaging Reviews*, vol. 19, no. 4, pp. 333–346, Apr. 2022, doi: 10.2174/1573405618666220610093740.
 - [29] A. Abbas, M. M. Abdelsamea, and M. M. Gaber, “Classification of COVID-19 in chest X-ray images using DeTraC deep convolutional neural network,” *Applied Intelligence*, vol. 51, no. 2, pp. 854–864, Feb. 2021, doi: 10.1007/s10489-020-01829-7.
 - [30] A. Agnihotri and N. Kohli, “(XAI-AGUWEM) Explainable Artificial Intelligence-based Attention Guided Uncertainty Weighting Ensemble Model for the Classification of COVID-19 and Pneumonia in X-ray Medical Images,” *Recent Advances in Electrical & Electronic Engineering (Formerly Recent Patents on Electrical & Electronic Engineering)*, vol. 18, no. 7, pp. 862–884, Aug. 2025, doi: 10.2174/0123520965334135241115064754.
 - [31] A. Hussain, S. U. Amin, H. Lee, A. Khan, N. F. Khan, and S. Seo, “An Automated Chest X-Ray Image Analysis for Covid-19 and Pneumonia Diagnosis Using Deep Ensemble Strategy,” *IEEE Access*, vol. 11, pp. 97207–97220, 2023, doi: 10.1109/ACCESS.2023.3312533.
 - [32] M. M. Kabir, M. F. Mridha, A. Rahman, M. A. Hamid, and M. M. Monowar, “Detection of COVID-19, pneumonia, and tuberculosis from radiographs using AI-driven knowledge distillation,” *Heliyon*, vol. 10, no. 5, pp. 1–16, Mar. 2024, doi: 10.1016/j.heliyon.2024.e26801.
 - [33] C. Randieri, A. Perrotta, A. Puglisi, M. G. Bocci, and C. Napoli, “CNN-Based Framework for Classifying COVID-19, Pneumonia, and Normal Chest X-Rays,” *Big Data and Cognitive Computing*, vol. 9, no. 7, pp. 1–18, Jul. 2025, doi: 10.3390/bdcc9070186.
 - [34] S. Q. Sabri, J. Y. Arif, G. A. Taqa, and A. Çınar, “A Comparative study of Chest Radiographs and Detection of The Covid 19 Virus Using Machine Learning Algorithm,” *Mesopotamian Journal of Computer Science*, vol. 2024, pp. 34–43, Mar. 2024, doi: 10.58496/MJCS/2024/004.
 - [35] E. M. F. El Houby, “COVID-19 detection from chest X-ray images using transfer learning,” *Scientific Reports*, vol. 14, no. 1, pp. 1–13, May 2024, doi: 10.1038/s41598-024-61693-0.




- [36] M. S. Hossain and M. Shorfuzzaman, "Noninvasive COVID-19 Screening Using Deep-Learning-Based Multilevel Fusion Model with an Attention Mechanism," *IEEE Open Journal of Instrumentation and Measurement*, vol. 2, pp. 1–12, 2023, doi: 10.1109/OJIM.2023.3303944.

BIOGRAPHIES OF AUTHORS



Girish Shyadanahalli Cheluvaraju    works as an assistant professor at the Department of Information Science and Engineering, GSSS Institute of Engineering and Technology for Women, Mysuru, India. He is doing his research (Ph.D.) in computer science and engineering at Visveswaraya Technological University, Belagavi. He has 11 years of teaching experience at both the UG and PG levels. His research interests include machine learning, artificial intelligence, image processing, and data science. He has published 4 technical papers and 5 book chapters. He has taught various courses, which include data structures, algorithms, C, C++, Java, Python, machine learning, data mining, discrete mathematics, microprocessors, graph theory, and software testing. He can be contacted at email: girishsadanahalli1127@gmail.com.



Dr. Jayasri Basavapatna Shivasubramanya    is currently working as a professor in the Department of Computer Science and Engineering at The National Institute of Engineering, Mysore, and Karnataka. She obtained her B.E. degree in CS (1997) from Mysore University and M.Tech. degree (2006) from Visveswaraya Technical University, Belgaum. She holds a Ph.D. in Computer Science and Engineering from NIE under VTU (July 2019). Her research primarily focuses on wireless sensor network. Has more than 24 years of teaching experience and has published more than 30 papers in reputed journal and conferences. Her area of interest includes wireless sensor networks, wireless communication, computer networks, operational research, and system simulation modelling. She can be contacted at email: jayasribs@nie.ac.in.